Application of attenuated total reflection Fourier transform infrared imaging and tape-stripping to investigate the three-dimensional distribution of exogenous chemicals and the molecular organization in *Stratum corneum*

Mila Boncheva
Firmenich SA Corporate R&D Division
PO Box 239
Route des Jeunes 1
CH-1211 Geneva 8 Switzerland

Feng H. Tay
Sergei G. Kazarian
Imperial College London
Department of Chemical Engineering
London SW7 2AZ United Kingdom

Abstract. Attenuated total reflection Fourier transform infrared spectroscopic imaging combined with tape-stripping is an advantageous approach to map the depth penetration and lateral distribution of topically applied chemicals in *Stratum corneum* (SC) and the conformational order of SC lipids. Tape-stripping progressively removes layers of SC, and chemical imaging provides spatially resolved information on the chemical composition of both the newly exposed SC surface and of the tapes used for stripping. The procedure is rapid, minimally invasive, and does not necessitate cross-sectioning of the skin. This approach offers a simple and direct way to determine the distribution of exogenous volatile and non-volatile chemicals in SC as a function of the chemical composition of the formulation and time, and the conformational order of SC lipids in native and topically treated skin. The procedure described here is well suited to address questions of relevance for the areas of drug delivery, dermatology, and skin care.
 [DOI: 10.1117/1.3006072]

Keywords: attenuated total reflection Fourier transform infrared imaging; drug delivery; skin; Stratum corneum; skin care; tape-stripping.

Paper 08192R received Jun. 20, 2008; revised manuscript received Jul. 29, 2008; accepted for publication Aug. 27, 2008; published online Nov. 10, 2008.

1 Introduction

The objective of this work was to develop a strategy for mapping the 3D distribution of chemicals in *Stratum corneum* (SC) following their topical application on the skin, and for studying their effect on the skin constituents. Here, we demonstrate the combined use of sequential tape-stripping of the SC surface and attenuated total reflection Fourier transform infrared (ATR-FTIR) imaging of both the newly exposed SC layers and of the tapes used for stripping. We applied this approach to follow the lateral distribution and penetration of the volatile and non-volatile ingredients of two model cosmetic formulations, Eau de toilette and cream, in excised skin, and to detect the changes induced in the conformational order of the SC lipids following their topical application.

The outermost skin layer, SC, is the principal target of topical cosmetic products and drugs and the main barrier for their penetration into the deeper skin layers, the viable epidermis and the dermis.[1,2] This layer, composed of terminally differentiated keratinocytes embedded in a lipid matrix, is highly inhomogeneous in its chemical composition and molecular organization in all three dimensions; the lateral and axial distributions of topically applied chemicals having different physicochemical properties in SC is, thus, inhomogeneous as well.[3–5] Knowledge of the chemical composition and structure of the native SC constituents and of the distribution of exogenous chemicals in all three dimensions is critical for improving the efficacy of topical formulations and for understanding the beneficial and undesirable side effects they might cause upon interaction with the SC lipids and proteins (e.g., reinforcing the SC barrier function and irritation or sensitization reactions).

The development of strategies for depth profiling of chemical species in the skin has been largely stimulated by the interest in developing systems for transdermal drug delivery (see, for example, Ref. 6, and the references therein). Tape-stripping, the sequential removal of SC layers using adhesive tapes, has been widely used in numerous pharmacological and dermatological applications.[7–9] The tapes used for stripping—containing ripped off SC material together with any exogenous chemical that may have penetrated into it—can be extracted and the chemical quantified by high-performance liquid chromatography (HPLC), gas chroatography (GC), scintillation counting, ultraviolet-visible (UV-vis), or infrared (IR) spectroscopy (for a recent review, see Ref.

Address all correspondence to: Mila Boncheva, Corporate R&D Division, Firmenich SA, PO Box 239, Route des Jeunes 1, CH-1211Geneva 8, Switzerland; Tel: (+41) 22 780 3027; E-mail: mila.boncheva@firmenich.com or to Sergei G. Kazarian, Imperial College London, Department of Chemical Engineering, London SW7 2AZ, United Kingdom; Tel: (+44) 207 594 5574; E-mail: s.kazarian@imperial.ac.uk

1083-3668/2008/13(6)/064009/7/$25.00 © 2008 SPIE

10). The depth distribution of chemical species within the SC—topically applied chemicals and SC components, such as lipids, proteins, water, and the constituents of the natural moisturizing factor—can be quantified also *in situ*, on the skin, using vibrational spectroscopic techniques: confocal Raman microspectroscopy as a stand-alone method[11–13] and ATR-FTIR spectroscopy (using horizontal ATR crystals[14–18] or fiber optical probes[19]) in combination with tape-stripping. Although these techniques are useful for comparing the relative amounts of chemical species present at various depths in the SC, they cannot provide information on the lateral distribution of the chemicals.

Chemical imaging and mapping of cells and tissues have been attracting increasing interest in the past two decades.[20] The strong background of spectra-structure correlations established in vibrational spectroscopy has enabled many new applications of chemical imaging in biomedical research,[20–22] including dermatology.[23,24] Using confocal Raman microscopy, chemical images of intact tissues can be acquired noninvasively to a depth of up to few hundred micrometers with a lateral resolution of up to ca. 1–2 μm and an axial resolution of ca. 2–5 μm.[25–27] The biggest disadvantages of the technique are the relatively long exposure times needed to map large surfaces[28,29] and the low signal-to-noise ratios (S/N). In contrast, FTIR imaging can be used to rapidly map bigger areas with up to ten times better S/N, but with a lower lateral resolution[30] (up to ca. 3–4 μm in ATR mode[31]). We have previously reported the usefulness of micro- and macro-ATR-FTIR imaging in studies of human SC.[31–33] Several other advanced analytical techniques (e.g., Fourier transform infrared photoacoustic spectroscopy,[34] near-infrared spectroscopy,[35] matrix-assisted laser desorption/ionization mass spectroscopy,[36] photothermal spectroscopy,[37] fluorescence life-time,[38] and infrared scanning near-field optical miscroscope[39]) have also been applied for skin imaging.

In most cases, skin imaging has been performed on cross-sectioned samples, thus implying the exclusive use of excised skin, access to microtoming equipment, and the possibility of introducing artifacts in the samples during their preparation (e.g., smearing chemicals during sectioning or modifying the tissue during the freezing or embedding procedures). The possibilities to construct 3D chemical maps of intact, living tissues have begun to emerge only recently.[33,40,41]

A recent publication from one of our labs reported a very promising combination of ATR-FTIR imaging with tape lifting;[42] there, we used FTIR imaging of adhesive tapes to detect the chemical composition of latent fingerprints. Here, we report the combined use of ATR-FTIR imaging and consecutive tape-stripping of SC to detect the lateral and axial distribution of exogenous chemicals and their influence on the conformational order of the lipid chains in SC. We applied ATR-FTIR imaging to construct chemical maps of surface layers of limited thickness (determined by the effective path length of the IR radiation) and tape-stripping to expose progressively deeper SC layers.

We first demonstrated the capability of our strategy for high-sensitivity detection of chemicals within the SC and compared spectra collected by a focal plane array (FPA) and a single-element detector from the tapes used for stripping of SC. Next, we applied ATR-FTIR imaging and tape-stripping to detect the time-dependent and formulation-dependent penetration of volatile and non-volatile chemicals into SC. Finally, we studied the depth profile of the conformational changes induced in SC lipids by a topically applied formulation.

The approach we propose is well suited to address questions of interest for the areas of transdermal drug delivery, dermatology, and skin care, such as the penetration profiles and the lateral distribution of topically applied chemicals (e.g., cosmetic ingredients, drugs, and airbome pollutants) and their influence on the organization of healthy, untreated skin.

2 Experimental

2.1 *Skin Samples*

We collected the ears of domestic pigs at the local slaughterhouse (Gland, Switzerland) 2–3 h after the animals were sacrificed. After thoroughly washing the ears with cold water, we removed the skin from the outer sides of the ears using a scalpel, clipped the hairs using hair clippers, and dermatomed the skin to a thickness of 350–400 μm using a 50-mm electric dermatome (Nouvag AG, Goldach, Switzerland). The skin was stored frozen at −20 °C (wrapped in Parafilm and packed in Ziploc®bags) for not longer than one month prior to use.

Before use, we defrosted the samples for 30 min at room temperature and wiped the SC surface two to three times with cotton swabs wetted with cold (4 °C) hexane, to remove traces of sebum.

2.2 *Model Cosmetic Formulations*

We used two simplified, model cosmetic formulations: Eau de toilette (EdT) and cream. EdT was prepared as 9:1 (v/v) ethanol/water solution, and the cream as water-in-oil emulsion of polyglyceryl esters, diesters, glycerol, fatty acids, and triglycerides. The two formulations contained 1% (w/v) of the volatile fragrance chemical 4-undecanolide (4U). We chose this elevated concentration (10–100 times higher than the typical concentrations of fragrance ingredients used in EdT and cream) to facilitate the spectroscopic detection of the chemical.

2.3 *Sample Preparation*

Before use, we equilibrated the skin samples clamped in static Franz diffusion cells for 2 h. The receptor compartments of the cells contained phosphate buffer solution (150 mM, pH 7.4) thermostated to maintain a temperature of 32 °C at the skin surface. We spread evenly the model formulations on the skin surface (5 μL/cm^2) using a Hamilton syringe and incubated the samples for 0.5, 2, or 4 h without occlusion at room temperature. At the end of the incubation period, we removed the skin samples from the diffusion cells and wiped off the excess formulation using a lint-free tissue.

2.4 *Tape-Stripping*

For this procedure, we used Scotch® packaging tape (3M) cut to size. After application of a piece of the tape onto the skin surface, we rolled a 2.8-kg metal cylinder over the tape ten times to ensure the homogeneous adhesion of the tape on the skin. We removed the tape in one rapid movement and, if necessary, repeated the stripping procedure using new pieces

of tape three or five times. For the imaging experiments, we used appropriately sized pieces of tape and skin (typically, with dimensions 5×5 mm) cut using a razor blade. We performed all experiments in triplicate.

2.5 *FTIR Spectroscopy and Imaging*

We performed the FTIR measurements using the setup described elsewhere[31,32] and a modified Golden Gate accessory (Specac Ltd.). We collected conventional FTIR spectra using a single-element mercury cadmium telluride (MCT) detector, and FTIR images—using a 64×64 FPA detector. The ATR imaging spectrometer is patented by Varian.[43] We collected the spectra with spectral resolution of 4 cm^{-1} in the spectral range of 3950–900 cm^{-1}. To obtain a reasonable S/N ratio, we co-added and averaged 64 scans. The acquisition time was ~90 s.

Unless otherwise indicated, we used the spectra without smoothing or baseline correction. We corrected the spectra of SC treated with cream (shown in Fig. 4) for the absorbance of the cream itself by subtracting the spectrum of pure cream from the combined spectrum until the spectral contribution of several vibrational bands characteristic for the cream—distinct from the bands originating from the skin and located in the fingerprint region—was minimized.

3 Results and Discussion

3.1 *ATR-FTIR Imaging of Stripping Tapes*

Figure 1 shows typical FTIR images of the fifth consecutive tape used for tape-stripping of SC following topical application of cream; Figure 1(a) maps the integrated absorbance of the Amide II band (1565–1500 cm^{-1}), corresponding to the lateral distribution of protein in the sample, and Figure 1(b) maps the integrated absorbance of the C–O stretching band (1080–1015 cm^{-1}), corresponding to the lateral distribution of the cream ingredients (e.g., glycerin, isopropyl myristate, polyglyceryl esters) in the sample. The polymer tapes and the SC lipids exhibited strong but overlapping CH_2 modes; consequently, in our imaging experiments we could not discern and map the distribution of SC lipids on tapes. The tapes, however, did not absorb in the typical for the SC proteins Amide I and II spectral regions; thus, in all FTIR images of tapes we used the distribution of the SC proteins (illustrated by the integrated absorbance of the Amide II band) to map the presence of skin flakes on the tapes.

The FTIR maps showed presence of both skin [Fig. 1(a)] and cream [Fig. 1(b)] on the tape, thus indicating that after four-hour topical application, a considerable amount of the cream has penetrated into the SC. As expected, the lateral distribution of the cream within the SC was highly inhomogeneous, ranging from areas containing large amounts (e.g., the points labeled A and B) to areas containing none (e.g., the point labeled C).

In Fig. 1(c), we compared spectra extracted from these three different spots of the ATR-FTIR images to the average spectrum collected from the entire sampled area using a single-element detector. As expected from the chemical maps, the two spectra A and B (which were extracted from areas with high local concentration of cream) showed strong absorption around 1040 cm^{-1}, the C–O stretching band originating from cream, while in spectrum C (which was extracted from an area containing no cream) this band was entirely missing. In spectrum MCT (the average spectrum collected from the sampled area), the C–O stretching band was extremely weak and almost invisible in the background of the C–C stretching modes originating from the skin itself; thus, if we had examined the heterogeneous tape sample using only a single-element detector, we would have arrived at the erroneous conclusion that only a minor amount of cream has penetrated into the SC down to the depth probed by the fifth tape.

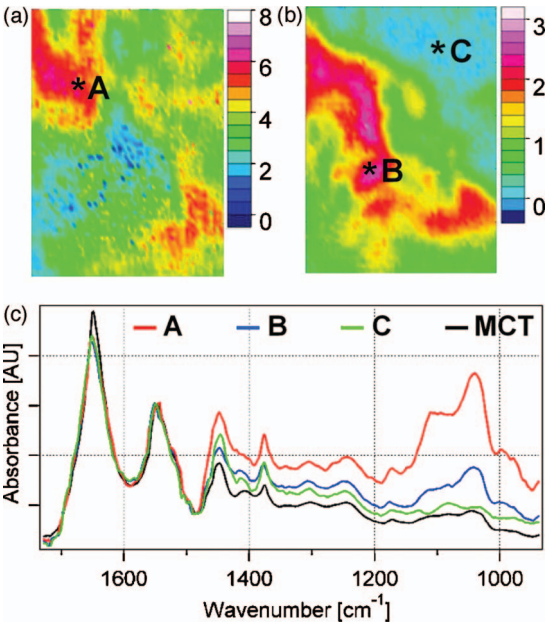

Fig. 1 ATR-FTIR imaging and spectroscopy of stripping tapes. FTIR images of the integrated absorbance of the Amide II band [1565–1500 cm^{-1}, (a)] and the C–O stretching band [1080–1015 cm^{-1} (b)] collected from the fifth consecutive tape used for stripping of porcine skin treated with cream for 4 h. The scales of the integrated absorbance shown next to the images use the same color coding (red for high intensity and blue for low intensity) but have different absolute values. Image dimensions: 500×700 μm. (c) IR spectra extracted from the points labeled A, B, and C in the IR images (shown respectively in red, blue, and green). The spectrum shown in black (labeled MCT) is the average spectrum collected from the imaged area using a single-element MCT detector. All spectra are baseline corrected and normalized to the maximal intensity of the Amide II band.

This comparison demonstrates that the use of FPA instead of single-element detection greatly increases the sensitivity of detection for samples with heterogeneous chemical composition,[44] an important consideration for the application of ATR-FTIR imaging to dermatological penetration studies.

3.2 *Time-Dependent Penetration of Non-volatile Chemicals into SC*

Figure 2 shows typical FTIR images of skin tape-stripped five times after topical treatment with cream for 0.5 and 4 h. The images map the lateral distribution of proteins using the integrated absorbance of the Amide II band [Figs. 2(a) and 2(b)] and of cream using the integrated absorbance of the C–O stretching band [Figs. 2(c) and 2(d)]. The maximum integrated absorbance of the Amide II found in the two samples was very similar [Figs. 2(a) and 2(b)]. The amount of cream

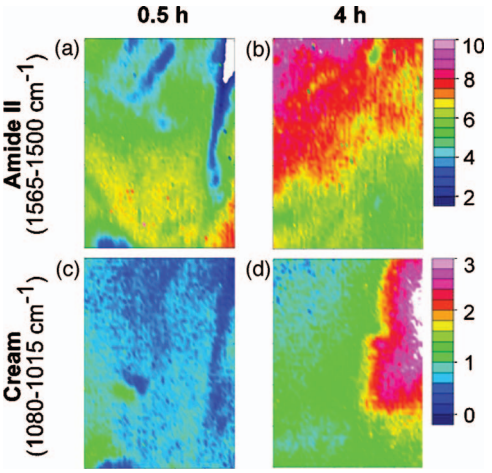

Fig. 2 Time-dependent skin penetration of non-volatile chemicals. FTIR images of the integrated absorbance of the Amide II band [1565–1500 cm^{-1}, (a, b)] and the C–O stretching band [1080–1015 cm^{-1}, (c, d)] collected from porcine skin treated with cream for 0.5 h (a, c) and 4 h (b, d) followed by five consecutive tape strips. The scales of the integrated absorbance shown next to the images use the same color coding (red for high intensity and blue for low intensity); the absolute values of the scale for (a) and (b) are different from those in the scale for (c) and (d). Image dimensions: 500 $\times$700 μm.

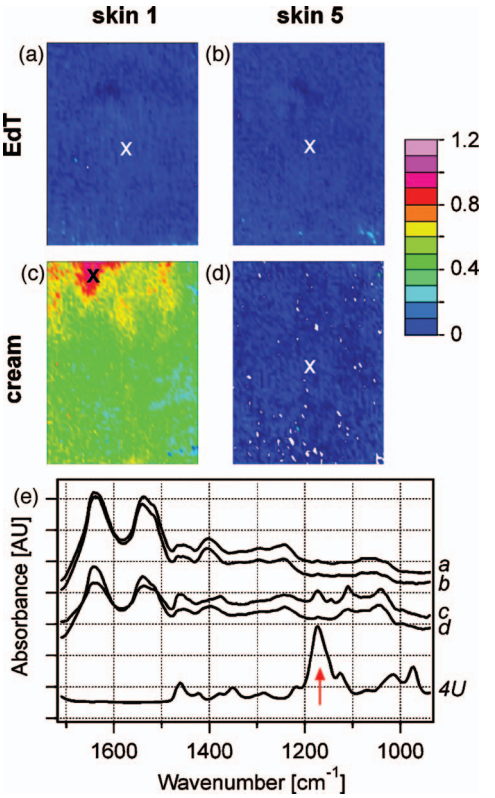

Fig. 3 Formulation-dependent retention of volatile chemicals in SC. (a–d) FTIR images of the integrated absorbance of the C–O–C stretching band (1200–1150 cm^{-1}) characteristic for 4U, collected from porcine skin treated with 4U-containing Eau de Toilette (a, b) and cream (c, d) for 0.5 h followed by one (a, c) or five (b, d) tape strips (denoted as skin 1 and skin 5, respectively). The color scale of the integrated absorbance is the same for all images. Image dimensions: 500 $\times$700 μm. (e) IR spectra extracted from the points marked in the IR images (labeled as the image from which they were extracted) and a spectrum from pure 4U. The arrow points to the C–O–C stretching vibration of 4U that was used to construct the images in a–d. The spectra are offset for clarity.

that had penetrated into the SC clearly showed the expected time dependence: both the area and the maximal absorbance of the cream-rich regions observed after 4 h treatment [Fig. 2(d)] were larger than those observed after 0.5 h treatment [Fig. 2(c)]. Thus, the combination of ATR-FTIR imaging and tape-stripping offers a simple and direct way to follow the penetration of chemicals into SC in semiquantitative, time-dependent studies *in situ*, avoiding the extraction of the stripping tapes needed in the traditional practice of tape-stripping.[10]

For the purposes of this work, we expressed the depth reached by the tape-stripping procedure within SC only in terms of number of tapes used for stripping of SC and not in terms of absolute distance below the SC surface. Although the present demonstration of principle can tolerate this approximation, it is important to keep in mind that the amount of SC material removed by one tape—and thus, the depth reached within the layer by tape-stripping—is not necessarily the same for all samples and depends on the relative depth within SC. In our future studies, we will quantify the amount of SC removed by each strip using, for example, gravimetric[15] or spectrophotometric[45] methods.

In principle, the approach we demonstrated here is also suitable to investigate the penetration pathways of chemicals into SC (e.g., their colocalization with the SC lipids or proteins). In the example shown in Fig. 2, the limited lateral resolution of the macro-imaging setup ($\sim$15 μm) precluded the possibility to map separately the SC proteins and lipids; these restrictions, however, can be easily surmounted using ATR-FTIR microscopy for imaging,[22] where the better lateral resolution (approximately 3–4 μm) could enable the resolution of lipid-rich and protein-rich regions.

3.3 *Formulation-Dependent Retention of Volatile Chemicals into the Topmost SC*

Next, we compared the amounts of the volatile fragrance chemical 4-undecanolide (4U) that have been retained within the topmost SC layers after treating the skin surface with two model cosmetic formulations, EdT and cream, each containing 1% (w/v) of 4U. Fig. 3 shows representative ATR-FTIR images of SC following topical application of the formulations for 0.5 h and tape-stripping the surface once [Fig. 3(a) and 3(c)] and five times [Figs. 3(b) and 3(d)]. The images map the integrated absorbance between 1200 and 1150 cm^{-1}, corresponding to the C-O-C stretching mode of 4U [indicated by arrow in Fig. 3(e)]. Figure 3(e) compares spectra extracted from the ATR-FTIR images with the spectrum of pure 4U.

In the sample treated with EdT, we could not detect 4U either in the topmost [Fig. 3(a)] or in the deeper SC layers [Fig. 3(b)]. This result indicated that, within the limit of detection of the instrument, the volatile fragrance chemical has evaporated completely during the period of unoccluded application, and it had not penetrated into the SC. In the sample treated with cream, we detected the presence of 4U only in the

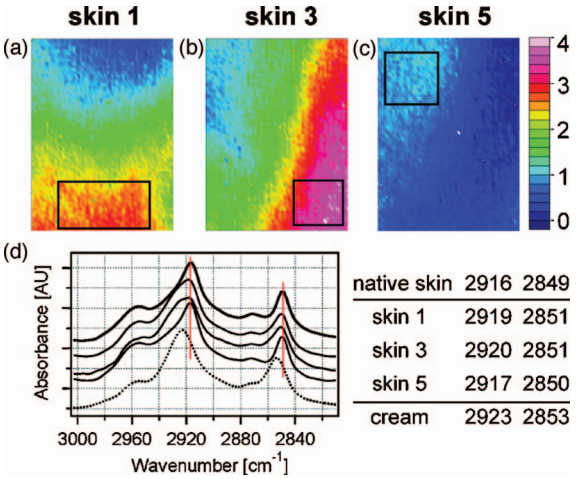

Fig. 4 Conformational order of SC lipids following topical treatment. (a–c) FTIR images of the integrated absorbance of the C–O stretching band (1080–1015 cm^{-1}) collected from porcine skin treated with cream for 2 h followed by (a) one, (b) three and (c) five consecutive tape strips (denoted as skin 1, skin 3, and skin 5, respectively). The scale of the integrated absorbance is the same for all images. Image dimensions: 500×700 μm. (d) IR spectra collected from untreated skin (thick line), extracted and averaged from the marked areas in the IR images (thin lines; a–c are plotted top to bottom), and collected from a cream sample (dotted line). The spectra extracted from the IR images were corrected for the absorbance of cream (see Experimental section for details). All spectra are baseline corrected, normalized to the maximal intensity of the CH_2 asymmetric stretching band, and offset for clarity. The vertical red lines indicate the positions of the CH_2 asymmetric and symmetric stretching bands in the spectrum of untreated skin. The positions of these bands in all spectra are tabulated next to the spectra.

topmost SC layer [Fig. 3(c)] but not in the deeper SC layers [i.e., those reached after five consecutive tape strips; Fig. 3(d)]. This result indicated that the cream had prevented the fast evaporation of 4U from the SC surface, most probably by an occlusive action. Even though the cream itself had penetrated into the deeper SC layers [see Fig. 2(d)] it did not, however, assist the penetration of the fragrance to this depth.

These experiments demonstrate that our strategy is well suited to address the relative effects of different formulations and application conditions on the balance between evaporation, retention, and penetration of volatile chemicals in the SC. It is, however, important to keep in mind that the utility of the methodology is subject to the sensitivity of detection of FTIR spectroscopy, which is inferior to the sensitivity that can be achieved using, for example, fluorescence or scintillation counting.

3.4 *Influence of Topically Applied Chemicals on the Conformational Order of SC Lipids*

The combination of tape-stripping and FTIR imaging is applicable also to detect the conformational changes that topically applied products induce in the lipid lamellae of SC. The images in Fig. 4 show the distribution of cream in the SC layers progressively revealed after stripping cream-treated skin with one [Fig. 4(a)], three [Fig. 4(b)], and five [Fig. 4(c)] tapes; to build the images we used the integrated absorbance between 1080–1015 cm^{-1}. In Fig. 4(d), we compared spectra extracted and averaged from the areas indicated on the images (after correcting them for the absorption of the cream itself; for details, see *Experimental* section) with an averaged spectrum collected from the surface of the SC before the application of cream and a spectrum collected from the cream sample.

The images in Figs. 4(a)–4(c) showed that the cream had penetrated into all studied SC layers following topical application for 2 h, with the highest absorbance observed after three tape strips. Concomitantly, the positions of the CH_2 symmetric and asymmetric stretching bands in the spectra of the cream-treated skin differed from those observed in the spectrum of untreated skin [Fig. 4(d)]. The magnitude of the blueshifts we observed correlated well with the relative amount of cream found in the samples, with the biggest shifts—of +4 and +2 cm^{-1} for the CH_2 asymmetric and symmetric stretching bands, respectively—found in the SC layer revealed after three tape strips. These results suggest that lipidic components from the cream got incorporated into the lipid matrix of the SC, which initially exhibited a high degree of conformational ordering as evidenced by the positions of the CH_2 stretching bands in this sample, and lead to its fluidization.

Thus, these experiments demonstrate that the combination of ATR-FTIR imaging and tape-stripping is well suited to study not only the presence of exogenous chemicals in the SC, but also the depth profile of the changes that they might inflict on the organization of the native SC lipids. Previous reports have shown that transmission FTIR imaging can be used to detect changes in the secondary structure of keratins in corneocytes isolated from stripping tapes.[16] The use of FTIR imaging in ATR mode might bring the additional advantage of performing such studies *in situ*, thus avoiding the need for isolation of the SC components from the stripping tapes.

4 Conclusions

This work describes the combined use of ATR-FTIR imaging and tape-stripping for mapping the lateral and axial distribution of exogenous chemicals in topically treated SC and the molecular organization of the SC lipids.

Our approach offers several advantages over the previously described methods. FTIR spectroscopic imaging using an FPA detector can deliver spatially resolved information on the chemical composition of heterogeneous samples with much higher sensitivity than possible using conventional spectroscopy, a technique that can deliver only spectra averaged over the entire sampled area. The depth resolution possible to achieve by ATR-FTIR imaging of tape-stripped skin is determined by the thickness of the SC layer removed by each tape and the thickness of the SC layer probed by the IR radiation (i.e., the IR effective pathlength). In our experimental setup, the effective pathlength varied between 1.4 and 2.8 μm (calculated using the Harrick's equation[46] while assuming a homogeneous incident angle of the IR beam equal to 45 deg and a refractive index of the skin equal to 1.5); this thickness was roughly equal to the thickness of the SC layer removed by one tape strip.[10] Thus, using the combination of ATR-FTIR imaging and tape-stripping, it is possible to rapidly build 3D chemical profiles of SC with an axial resolution comparable to the one that can be achieved by confocal Raman imaging

but with a better S/N. This strategy avoids the inconveniences linked to the customary techniques for sample preparation (e.g., possible smearing and material transfer during microtoming of the sample and artifacts due to freezing of the samples or the different embedding procedures) and the isolation of SC components from the tapes. The imaging can be performed not only on the skin sample, but also on the tapes used for stripping; thus, the collection of samples and the consequent imaging can be preformed at different locations. The minimal invasiveness of the procedure and the short collection times are, in principle, appropriate for *in vivo* application.

Our strategy bears also the limitations typical of all FTIR-based methodologies. It is suitable only for detection of molecules containing IR-active vibrational modes, ideally ones that do not overlap with modes originating from the native skin components; the use of deuterated chemicals can greatly facilitate the analysis of the spectral information.[16] The quantitative interpretation of ATR chemical images of skin is often challenging, and the method has lower sensitivity of detection than some of the other techniques that can be used in conjunction with tape-stripping (e.g., HPLC or GC). Unlike ATR imaging, however, these techniques cannot deliver spatially resolved information on the chemical composition and structure of the samples.

We believe that the strategy presented in this work will contribute to the development of techniques for assessment of the risks and benefits associated with the topical application of cosmetic products and drugs, and for understanding the penetration pathways of exogenous chemicals through SC.

Acknowledgments

This study was supported by Firmenich SA. F. H. Tay and S. G. Kazarian thank EPSRC for support (EP/D502721).

References

1. J. A. Bouwstra and M. Ponec, "The skin barrier in healthy and diseased state," *Biochim. Biophys. Acta* **1758**, 2080–2095 (2006).
2. K. C. Madison, "Barrier function of the skin: "La raison d'être" of the epidermis," *J. Invest. Dermatol.* **121**, 231–241 (2003).
3. D. T. Downing, "Lipid and protein structures in the permeability barrier of mammalian epidermis," *J. Lipid Res.* **33**, 301–313 (1992).
4. B. Forslind, "A domain mosaic model of the skin barrier," *Acta Derm. Venereol.* **74**, 1–6 (1994).
5. C. R. Harding, "The Stratum corneum: structure and function in health and disease," *Dermatol. Therapy* **17**, 6–15 (2004).
6. M. R. Prausnitz, S. Mitragotri, and R. Langer, "Current status and future potential of transdermal drug delivery," *Nat. Rev. Drug Discovery* **3**, 115–124 (2004).
7. A. Rougier and C. Lotte, "Predictive approaches I. The stripping technique," in *Topical Drug Bioavailability, Bioequivalence, and Penetration*, V. P. Shah and H. I. Maibach, Eds., pp. 163–181, Plenum, New York (1993).
8. W. Diembeck, H. Beck, F. Benech-Kieffer, P. Courtellemont, J. Dupuis, W. Lovell, M. Paye, J. Spengler, and W. Steiling, "Test guidelines for *in vitro* assessment of dermal absorption and percutaneous penetration of cosmetic ingredients," *Food Chem. Toxicol.* **37**, 191–205 (1999).
9. C. C. Dary, J. N. Blancato, and M. A. Saleh, "Chemomorphic analysis of malathion in skin layers of the rat: Implications for the use of dermatopharmacokinetic tape-stripping in exposure assessment to pesticides," *Regul. Toxicol. Pharmacol.* **34**, 234–248 (2001).
10. C. Herkenne, I. Alberti, A. Naik, Y. N. Kalia, F.-X. Mathy, V. Preat, and R. H. Guy, "*In vivo* methods for the assessment of topical drug bioavailability," *Pharm. Res.* **25**, 87–103 (2007).
11. P. J. Caspers, G. W. Lucassen, E. A. Carter, H. A. Bruining, and G. J. Puppels, "*In vivo* confocal Raman microspectroscopy of the skin: Non-invasive determination of molecular concentration profiles," *J. Invest. Dermatol.* **116**, 434–442 (2001).
12. P. D. A. Pudney, M. Melot, P. J. Caspers, A. van der Pol, and G. J. Puppels, "An *in vivo* confocal Raman study of the delivery of trans-retinol to the skin," *Appl. Spectrosc.* **61**, 804–811 (2007).
13. M. Egawa, T. Hirao, and M. Takahashi, "*In vivo* estimation of Stratum corneum thickness from water concentration profiles obtained with Raman spectroscopy," *Acta Derm. Venereol.* **87**, 4–8 (2007).
14. A. L. Stinchcomb, F. Pirot, G. D. Touraille, A. L. Bunge, and R. H. Guy, "Chemical uptake into human Stratum corneum *in vivo* from volatile and non-volatile solvents," *Pharm. Res.* **16**, 1288–1293 (1999).
15. A. Naik and R. H. Guy, "Infrared spectroscopic and differential scanning calorimetric investigations of the Stratum corneum barrier function," in *Mechanisms of Transdermal Drug Delivery*, R. O. Potts and R. H. Guy, Eds., Marcel Dekker, New York (1997).
16. R. Mendelsohn, C. R. Flach, and D. J. Moore, "Determination of molecular conformation and permeation in skin via IR spectroscopy, microscopy, and imaging," *Biochim. Biophys. Acta* **1758**, 923–933 (2006).
17. M. Boncheva, F. Damien, and V. Normand, "Molecular organization of the lipid matrix in intact Stratum corneum using ATR-FTIR spectroscopy," *Biochim. Biophys. Acta* **1778**, 1344–1355 (2008).
18. M. Dias, A. Naik, R. H. Guy, J. Hadgraft, and M. Lane, "*In vivo* infrared spectroscopy studies of alkanol effects on human skin," *Eur. J. Pharm. Biopharm.* **69**, 1171–1175 (2008).
19. H. M. Heise, L. Kuepper, W. Pittermann, and L. N. Butvina, "New tool for epidermal and cosmetic formulation studies by ATR spectroscopy using a flexible mid-infrared fiber probe," *Fresenius' J. Anal. Chem.* **371**, 753–757 (2001).
20. R. Bhargava and I. W. Levin, *Spectrochemical Analysis Using Infrared Multichannel Detectors*, Blackwell, Oxford, UK (2005).
21. See the collection of papers presented at SPEC'04 and SPEC'06, published respectively in *Vibrational Spectroscopy* 38 (2005) and *Biochim. Biophys. Acta* **1758** (2006).
22. S. G. Kazarian and K. L. A. Chan, "Application of ATR-FTIR spectroscopic imaging to biomedical samples," *Biochim. Biophys. Acta* **1758**, 858–867 (2006).
23. R. Mendelsohn, H.-C. Chen, M. E. Rerek, and D. J. Moore, "Infrared microspectroscopic imaging maps the spatial distribution of exogenous molecules in skin," *J. Biomed. Opt.* **8**, 185–190 (2003).
24. G. Zhang, D. J. Moore, C. R. Flach, and R. Mendelsohn, "Vibrational microscopy and imaging of skin: from single cells to intact tissues," *Anal. Bioanal. Chem.* **387**, 1591–1599 (2007).
25. C. Krafft and V. Sergo, "Biomedical application of Raman and infrared spectroscopy to diagnose tissues," *Spectroscopy* **20**, 195–218 (2006).
26. C. Matthaeus, S. Boydston-White, M. Miljkovic, M. Romeo, and M. Diem, "Raman and infrared microspectral imaging of mitotic cells," *Appl. Spectrosc.* **60**, 1–8 (2006).
27. S. Schluecker, M. D. Schaeberle, S. W. Huffman, and I. W. Levin, "Raman microspectroscopy: a comparison of point, line, and wide-field imaging methodologies," *Anal. Chem.* **75**, 4312–4318 (2003).
28. G. Zhang, D. J. Moore, K. B. Sloan, C. R. Flach, and R. Mendelsohn, "Imaging the prodrug-to-drug transformation of a 5-fluorouracil derivative in skin by confocal Raman microscopy," *J. Invest. Dermatol.* **127**, 1205–1209 (2007).
29. G. Zhang, C. R. Flach, and R. Mendelsohn, "Tracking the dephosphorylation of resveratrol triphosphate in skin by confocal Raman microscopy," *J. Controlled Release* **123**, 141–147 (2007).
30. P. Lasch and D. Naumann, "Spatial resolution in infrared microspectroscopic imaging of tissues," *Biochim. Biophys. Acta* **1758**, 814–829 (2006).
31. K. L. A. Chan and S. G. Kazarian, "New opportunities in micro- and macro-ATR infrared spectroscopic imaging: Spatial resolution and sampling versatility," *Appl. Spectrosc.* **57**, 381–389 (2003).
32. K. L. A. Chan and S. G. Kazarian, "Chemical imaging of *Stratum corneum* under controlled humidity with ATR-FTIR spectroscopy method," *J. Biomed. Opt.* **12**, 044010 (2007).
33. K. L. A. Chan and S. G. Kazarian, "ATR FTIR imaging with variable angle of incidence: A three-dimensional profiling of heterogeneous materials," *Appl. Spectrosc.* **61**, 48–54 (2007).
34. S. Wartewig and R. H. H. Neubert, "Pharmaceutical applications of mid-IR and Raman spectroscopy," *Adv. Drug Delivery Rev.* **57**,

1144–1170 (2005).
35. S. L. Zhang, C. L. Meyers, K. Subramanyan, and T. M. Hancewicz, "NIR imaging for measuring and visualizing skin hydration: A comparison with visual assessment and electrical methods," *J. Biomed. Opt.* **10**, 031107 (2005).
36. J. Bunch, M. R. Clench, and D. S. Richards, "Determination of pharmaceutical compounds in skin by imaging MALDI-MS," *Rapid Commun. Mass Spectrom.* **18**, 3051–3060 (2004).
37. R. D. Snook, R. D. Lowe, and M. L. Baesso, "Photothermal spectrometry for membrane and interfacial region studies," *Analyst* **123**, 587–593 (1998).
38. R. Niesner, B. Peker, P. Schluesche, K.-H. Gericke, C. Hoffmann, D. Hahne, and C. Mueller-Goymann, "3D-resolved investigation of the pH gradient in artificial skin constructs by means of fluorescence lifetime imaging," *Pharm. Res.* **22**, 1079–1087 (2005).
39. A. Cricenti, R. Generosi, M. Luce, P. Perfetti, G. Margaritondo, D. Talley, J. S. Sanghera, I. D. Aggarwal, N. H. Tolk, A. Congiu-Castellano, M. A. Rizzo, and D. W. Piston, "Chemically resolved imaging of biological cells and thin films by infrared scanning near-field optical microscopy," *Biophys. J.* **85**, 2705–2710 (2003).
40. See, for example, the invited lectures of the 1st Int. Workshop on Spectral Diagnostics (SD-1), Boston, MA, June 21–23, 2007 ⟨https://spectraldiagnosis.com/⟩.
41. C. Ricci, K. L. A. Chan, and S. G. Kazarian, "Combining the tape-lift method and FTIR imaging for forensic applications," *Appl. Spectrosc.* **60**, 1013–1021 (2006).
42. C. Ricci, S. Bleay, and S. G. Kazarian, "Spectroscopic imaging of latent fingermarks collected with the aid of a gelatin tape," *Anal. Chem.* **79**, 5771–5776 (2007).
43. E. M. Burka and R. Curbelo, "ATR imaging spectrometer," U.S. patent No. 6,141,100 (2000).
44. K. L. A. Chan and S. G. Kazarian, "Detection of trace materials with Fourier transform infrared spectroscopy using a multichannel detector," *Analyst* **131**, 126–131 (2006).
45. R. Voegeli, J. Heiland, S. Doppler, A. V. Rawlings, and T. Schreier, "Efficient and simple quantification of Stratum corneum proteins on tape strippings by infrared densitometry," *Skin Res. Technol.* **13**, 242–251 (2007).
46. N. J. Harrick, "Internal reflection spectroscopy," Harrick Scientific Corporation, New York (1987).